Pinholes and temperature-dependent transport properties of MgO magnetic tunnel junctions

J. Ventura,* J. M. Teixeira, J. P. Araujo, and J. B. Sousa
Faculty of Sciences and IN, IFIMUP unit, Universidade do Porto, Rua do Campo Alegre, 678, 4169-007, Porto, Portugal

P. Wisniowski and P. P. Freitas
IN, INESC MN unit, Rua Alves Redol, 9-1, 1000-029 Lisbon, Portugal
(Received 24 March 2008; published 2 July 2008)

Magnetic tunnel junctions (MTJs) with thin crystalline MgO(001) barriers displaying large tunnel magnetoresistance (TMR) and low resistance-area product (*RA*) will likely be used as the next generation sensors in read heads of ultrahigh-density hard drives. However, the thin insulating barrier may result in the presence of metallic pinholes joining the two electrodes. Here we study the transport properties of thin MgO-based low resistance MTJs (barrier thickness $t=7.5$ Å), deposited by magnetron sputtering, with *RA* values of $\sim 40\ \Omega\mu m^2$, reaching TMR values of $\sim 60-75\%$ at room temperature. We performed temperature-dependent (300–20 K) resistance (R) measurements and observed different behaviors for different magnetic states: positive dR/dT for the parallel (P) state, attributed to the presence of pinholes in the barrier, but a mixed character in the antiparallel (AP) state, with dR/dT changing from negative to positive with decreasing temperature. This indicates an interesting competition between tunneling and metallic transport in the studied samples. To explain this transport behavior, we developed a simple model with the two conducting channels, tunnel and metallic, in parallel. The model assumes a linear variation of the electrical resistance with temperature for both conducting channels and its dependence on the MTJ magnetic state (P and AP). The modeled results show that the sign of dR/dT does not give an indication of the dominant conductance mechanism and that the crossover temperature at which dR/dT changes sign depends strongly on the linear electrical resistance–temperature coefficients. We performed fits to our experimental $R(T)$ data, using the proposed model, and observed that such fits reproduced the data quite well, illustrating the validity of the model.

DOI: 10.1103/PhysRevB.78.024403 PACS number(s): 73.40.Rw, 85.30.Mn, 73.43.Qt, 73.63.−b

I. INTRODUCTION

Magnetic tunnel junctions (MTJs),[1,2] constituted by two ferromagnetic (FM) layers separated by an insulating barrier, are currently used as magnetic sensors in high-density recording media.[3,4] The characteristics of the tunnel junctions implemented in read heads include a low resistance-area product (*RA*), for achieving a high readout speed and a high enough sensitivity to read the ever smaller magnetic bit. To achieve the desired *RA* values, the thickness of the insulating barrier is decreased to less than 1 nm, toward a few atomic planes thick. This leads to the possible existence of metallic paths across the insulating barrier (pinholes), with consequences in device reproducibility, performance, and reliability.[5,6] Furthermore, the presence of pinholes can have an important impact on the MTJ-spin-transfer driven magnetization dynamics,[7] or on the MTJ-magnetoresistance sign.[8]

Recently, tunnel junctions with crystalline MgO(001) barriers[9,10] displaying very large tunnel magnetoresistance (TMR) ratios were successfully fabricated,[11–14] opening new opportunities to develop read heads for ultrahigh-density hard drives. The large TMR ratio of crystalline MgO tunnel junctions arises from the different symmetry-related decay rates of the Bloch waves for majority- and minority-spin channels.[15,16] For sensor applications, MTJs with tunnel magnetoresistance above 50% and *RA* as low as 0.4 $\Omega\mu m^2$ were recently obtained using thin MgO barriers.[17] However, a significant TMR decrease is usually observed with decreasing MgO thickness,[18] showing the importance of studying the impact of pinholes on the magnetotransport properties of ultrathin magnetic tunnel junctions.

To probe the absence of pinholes in MTJs, one usually uses the three applicable Rowell criteria.[19] However, both the exponential dependence of resistance on insulator thickness and the nonlinear current-voltage characteristics were found to be nonreliable even in high resistance tunnel junctions ($RA \gtrsim 1\ k\Omega\mu m^2$).[20,21] On the other hand, the third criterion [the weak insulatinglike temperature dependence of the electrical resistance ($dR/dT<0$)], although insensitive to the presence of few or small pinholes in low resistance MTJs ($\lesssim 10\ \Omega\mu m^2$),[22,23] can be used to probe the presence of sizable pinholes in the barrier.[24]

Here we study the temperature dependence (300–20 K) of the transport properties of low resistance magnetic tunnel junctions with an ultrathin MgO barrier (7.5 Å). Our samples display $RA \sim 40\ \Omega\mu m^2$ and TMR $\sim 60-75\%$ at room temperature. Temperature-dependent electrical resistance measurements [$R(T)$] allowed us to observe different behaviors depending on the MTJ magnetic state. The studied samples showed positive dR/dT for the parallel (P) state, indicating a metalliclike behavior, so that pinholes are already present in the barrier. However, in the antiparallel (AP) state, the $R(T)$ curves exhibit a mixed character, with dR/dT negative at sufficiently high temperatures but changing to positive at low temperatures. These results show an interesting competition between tunnel and metallic transport in the studied samples.

In order to understand this transport behavior, we propose a simple model of two conducting channels, metallic and tunnel, acting in parallel. We assume a linear temperature variation of the electrical resistance for both conducting channels, as observed experimentally over a broad tempera-

ture range. The model also takes into account the experimentally observed dependence of the linear coefficients on the MTJ magnetic state (parallel and antiparallel). According to the model, the sign of the dR/dT derivative does not illustrate the dominant conductance mechanism and the crossover temperature (T^*) at which dR/dT changes sign in the AP state depends strongly on the linear temperature coefficients. Fittings performed to the experimental $R(T)$ data, using the developed model, reproduce the data quite well, illustrating the validity of the model.

II. EXPERIMENTAL DETAILS

A set of thin MTJs was deposited at INESC MN in a Nordiko 2000 magnetron sputtering system with base pressure of 7×10^{-9} Torr in dc and rf (CoFe and MgO) modes. The structure of the deposited MTJs was glass/Ta (50 Å)/Ru (180 Å)/Ta (30 Å)/MnPt (200 Å)/CoFe (22 Å)/Ru (9 Å)/CoFeB (30 Å)/MgO (7.5 Å)/CoFeB (30 Å)/Ru (50 Å)/Ta (50 Å). The MgO barrier was directly deposited from a stoichiometric MgO single-crystal target. The compositions of the magnetic compound are $Co_{82}Fe_{18}$, $(Co_{52}Fe_{48})_{75}B_{25}$, and $Pt_{46}Mn_{54}$. During deposition a magnetic field of 20 Oe was applied to define the magnetic anisotropy axes of the pinned and free layers in the same direction. Before the patterning process, the structure was covered with 150 Å of $Ti_{10}W_{90}(N_2)$, also deposited by magnetron sputtering. Magnetic tunnel junctions were then microfabricated by optical lithography and ion-beam milling in a rectangular shape with areas of 2×4 μm^2. The low resistance of the leads enabled uniform current flow over the tunnel junction area.[25] Patterned samples were annealed in high vacuum at 613 K for 1 h in a magnetic field of 5 kOe applied along the easy axis.

Electrical resistance and magnetoresistance were measured with a four-point dc method, with a current stable to $1:10^6$ and using an automatic control and data acquisition system. Temperature-dependent measurements were performed in a closed cycle cryostat down to 20 K.[26,27] We define here the relative MTJ-resistance change (for parallel and antiparallel states) between 300 and 20 K as $\gamma_{P,AP}=(R^{P,AP}_{300\ K}-R^{P,AP}_{20\ K})/R^{P,AP}_{300\ K}$, so that $\gamma<0$ (>0) indicates tunnel- (metallic-) like transport.[24]

III. EXPERIMENTAL RESULTS

The temperature dependence (300–20 K) of the electrical resistance $R(T)$ and magnetoresistance MR(T) of two magnetic tunnel junctions of the same series (7.5 Å barrier thickness; deposited and microfabricated together) is shown in Fig. 1. Magnetoresistance cycles for the studied samples gave MR $\sim$60–75 % at room temperature (inset of Fig. 1), with $RA\sim40$ $\Omega\mu m^2$. We observed that the magnetoresistance of the studied samples increased with decreasing temperature,[28] reaching $\sim$75–90 % at low temperatures (inset of Fig. 1).

Figure 1 shows that our samples have different $R(T)$ behaviors depending on their magnetic state (parallel or antiparallel). Both samples 1 ($RA\sim38$ $\Omega\mu m^2$) and 2 (RA

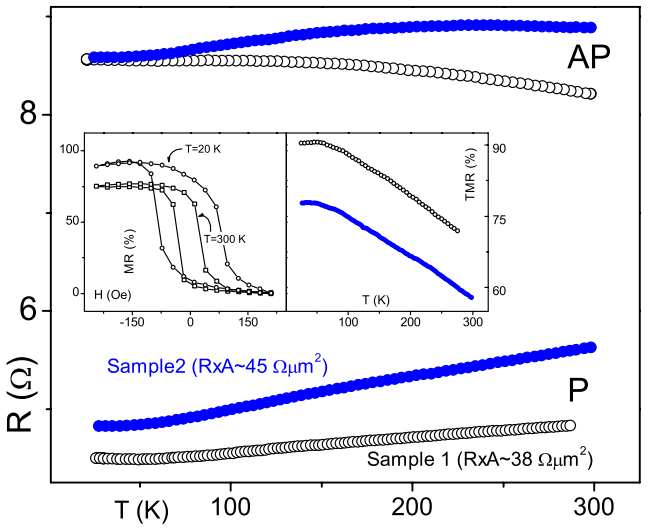

FIG. 1. (Color online) Temperature dependence of the electrical resistance of samples 1 and 2 in the parallel and antiparallel states. Insets: Room- and low-temperature magnetoresistance cycles (sample 1) and MR temperature dependence.

~45 $\Omega\mu m^2$) show positive dR/dT for the parallel state ($\gamma_P=7.0\%$ and $\gamma_P=9.3\%$, respectively), typical of a metallic behavior, so that metallic conductance channels (pinholes across the barrier) are already present in the barrier.[22] An overall small negative relative MTJ-resistance change was observed for the AP state in sample 1 ($\gamma_{AP}=-4\%$) but a positive one for sample 2 ($\gamma_{AP}=4\%$). These results clearly evidence the existence of a competition between tunnel and metallic transport in the studied magnetic tunnel junctions.[24] In particular, one has two conductance channels acting in parallel in our MTJs: tunneling through the thin MgO barrier and metallic transport across pinholes in the barrier. The slight differences in the $R(T)$ behaviors of the two magnetic tunnel junctions are likely due to differences in the average barrier properties over the junction area (fluctuations in the barrier thickness of the ultrathin MgO film or number and size of pinholes present in the barrier).

Two main differences are seen in the parallel and antiparallel $R(T)$ curves. In the parallel state, $R^P(T)$ clearly exhibits the standard metallic linear behavior from intermediate to high temperatures, suggesting electron-phonon scattering (e.g., s-s induced electron transitions in typical metals such as Cu, plus s-d scattering in transition metals). This is further confirmed in Fig. 2(a), where we display the temperature derivative of the normalized electrical resistance, $(dR/dT)/(R_{300\ K}-R_0)$ (where R_0 is the minimum resistance of each sample). These curves indeed resemble the normalized Bloch-Grüneisen prediction associated with electron-phonon scattering in s-d transition metals.[29]

On the other hand, in the AP state the R^{AP}(T) curves exhibit a mixed character, with dR/dT negative at sufficiently high temperatures but getting positive as the temperature decreases [at $T^*\approx90$ and 240 K for samples 1 and 2, respectively; see arrows in Fig. 2(b)]. However, since a positive dR^P/dT is observed, one would expect such metallic conductance to be visible in the AP state in all the studied temperature range (since the tunnel resistance switches to a higher

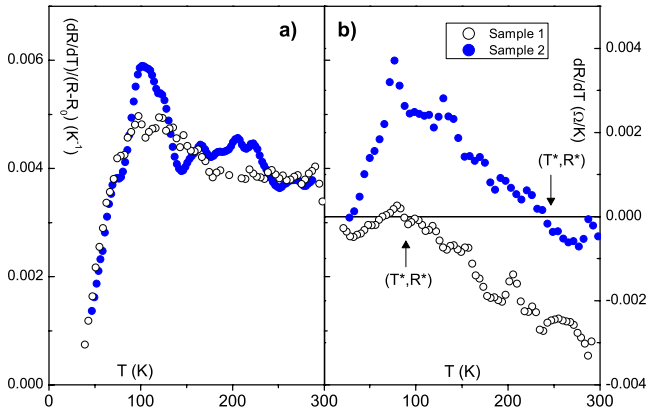

FIG. 2. (Color online) Temperature derivative of (a) the normalized electrical resistance in the parallel state and (b) the electrical resistance in the antiparallel state.

value). The observation of a negative dR/dT for the AP configuration at sufficiently high temperatures must therefore be understood.

IV. MODEL

To model our temperature-dependent transport data, we naturally start by considering tunnel and metallic conductance channels acting in parallel with resistances R_t and R_m, respectively. The equivalent resistance (R) is then given by

$$\frac{1}{R(T)} = \frac{1}{R_m(T)} + \frac{1}{R_t(T)}. \tag{1}$$

One has now to consider the R_t and R_m temperature variations. Let us assume linear variations with temperature for both cases, with coefficients α_t and α_m for the tunnel and metallic channels, respectively. One can then write

$$R_t(T) = R_{t_0} - \alpha_t T, \tag{2}$$

and

$$R_m(T) = R_{m_0} + \alpha_m T, \tag{3}$$

where R_{t_0} and R_{m_0} are the (extrapolated) tunnel and metallic resistances at zero temperature.

Within this simple model, the condition that determines the metalliclike $R(T)$ behavior ($dR/dT > 0$) is given by

$$\frac{R_t(T)}{\sqrt{\alpha_t}} > \frac{R_m(T)}{\sqrt{\alpha_m}}. \tag{4}$$

An insulatorlike behavior is found if the above inequality, with the reverse sign, is fulfilled. One immediately realizes that if α_t is sufficiently higher than α_m, one can even observe insulatorlike behavior ($dR/dT < 0$) with a tunnel resistance larger than the metallic resistance (or vice versa). Note that this contrasts with what one would intuitively assume, that such crossover would occur when the metallic and insulator resistances are similar and that a metallic $R(T)$ behavior immediately implies lower resistance of the metallic nanoconstrictions.

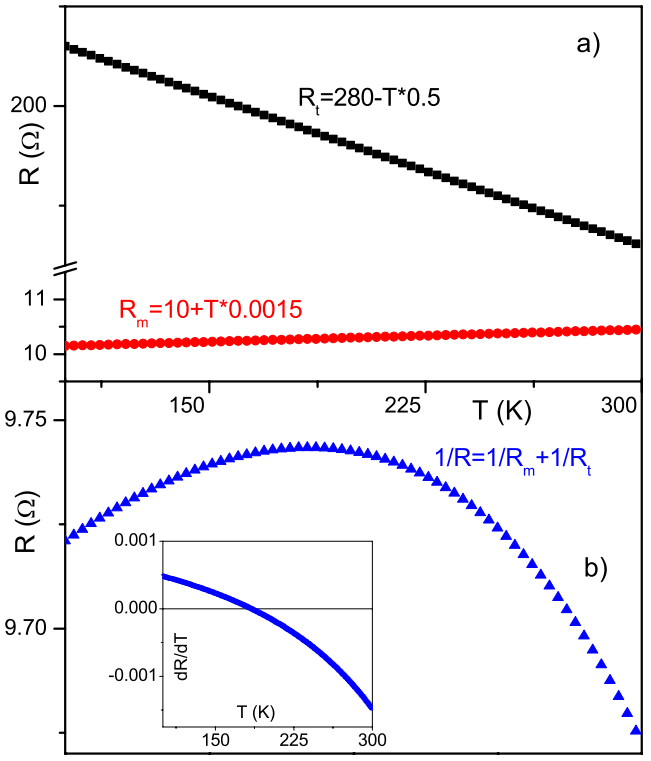

FIG. 3. (Color online) (a) Simulated R_m and R_t curves using Eqs. (2) and (3) and the parameters mentioned in the text. (b) Equivalent resistance $R^{-1} = R_m^{-1} + R_t^{-1}$. Inset: Temperature derivative of the equivalent resistance, showing a change of sign at $T^* \approx 185$ K.

The crossover temperature T^* and crossover resistance R^* can be found using this simple model, giving

$$T^* = \frac{R_{t_0}\sqrt{\alpha_m} - R_{m_0}\sqrt{\alpha_t}}{\alpha_t\sqrt{\alpha_m} + \alpha_m\sqrt{\alpha_t}}, \tag{5}$$

and

$$R^* = \frac{\sqrt{\alpha_t\alpha_m}}{\sqrt{\alpha_m} + \alpha_m}\frac{R_{t_0}\alpha_m + R_{m_0}\alpha_t}{\alpha_t\sqrt{\alpha_m} + \alpha_m\sqrt{\alpha_t}}. \tag{6}$$

In Fig. 3 we plot the modeled $R_t(T)$, $R_m(T)$, and $R(T)$ curves with the example parameters $R_{t_0} = 280\ \Omega$ (the resistance obtained using the Simmons model with a barrier thickness $t = 7.5$ Å, a barrier height $\phi \approx 1.4$ eV, and $A = 8\ \mu\text{m}^2$), $\alpha_t = 0.5\ \Omega/\text{K}$ (see below), $R_{m_0} = 10\ \Omega$ (corresponding approximately to a circular metallic spin valve with a diameter $d \sim 0.15\ \mu$m),[30] and $\alpha_m = 1.5\ \text{m}\Omega/\text{K}$ (also inferred from Ref. 30). We clearly see that, although $R_m \ll R_t$ for all the simulated T range [Fig. 3(a)], there is a crossover to negative dR/dT at $T^* \approx 185$ K [Fig. 3(b) and inset, where dR/dT is plotted]. This is related to the large differences in the α_t and α_m values.

Figure 4 shows that (model) changes in the $\alpha_{m,t}$ parameters lead to shifts in the positive to negative dR/dT crossover temperature. Increasing α_m [Fig. 4(a)] leads to the increase in T^*, while for increasing α_t [Fig. 4(b)], T^* decreases. Note, however, that in all the simulated cases we have R_m

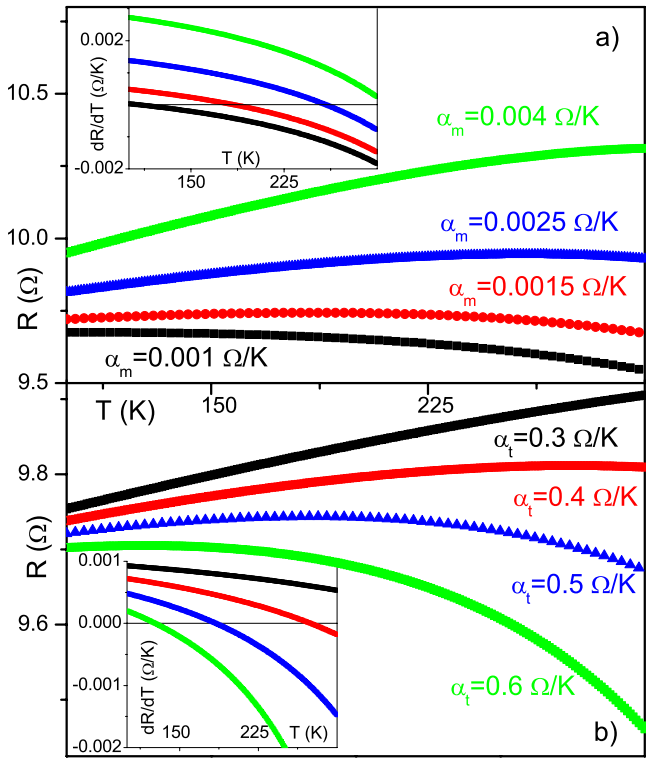

FIG. 4. (Color online) Effect of the variation of (a) α_m and (b) α_t on the equivalent resistance R. Insets: Corresponding temperature derivatives. Notice how small changes in these parameters can lead to a significant variation of the crossover temperature T^*.

$\ll R_t$ (note that $R_{t_0}=280\ \Omega$ and $R_{m_0}=10\ \Omega$). These results then show that the sign of the dR/dT derivative does not give an indication of the dominant conductance mechanism.

The assumption of linear $R_{m,t}(T)$ behaviors must now be justified. First, the thermal dependence of the tunnel resistance is usually considered to arise from several origins:

(i) The usual decrease in the ferromagnet magnetization (M) with temperature, due to the thermal excitation of magnons. The spin polarization P is then assumed to vary as M and Juliere's model[31] can be extended to account for such T dependence.[28,32–34]

(ii) Hopping through localized states in the barrier.[32]

(iii) The excitation of magnons at the FM/barrier interface,[35–37] also proposed as source of the temperature dependence of the tunnel resistance.

However, in spite of the above referred complex contributions, a fairly linear relation is experimentally observed in the $R(T)$ curves of thick MgO magnetic tunnel junctions over a broad temperature range (from below $\sim$100 K to room temperature; see, e.g., Ref. 37).

Regarding R_m, we notice that a linear relation with temperature (at least near room temperature) is usual for common metals and is indeed observed in CoFe/Cu/CoFe spin valves for $T \gtrsim 100$ K.[38] Therefore, the approximation of linear $R_{m,t}(T)$ behaviors should be valid in a broad range of temperatures, ranging from below $\sim$100 K to room temperature. The analysis of our experimental data below will then be restricted to such limited range.

Taking into account our experimental data, we will now concentrate on the inversion of the dR/dT sign visible for the AP state (at a temperature T^* and a resistance R^*). Taking the temperature derivative of Eq. (1), one can relate the easily detected inversion point (T^*,R^*) coordinates with the R_{t_0,m_0} model parameters, getting

$$R_{t_0} = R^*\left(1 + \sqrt{\frac{\alpha_t}{\alpha_m}}\right) + \alpha_t T^*, \tag{7}$$

and

$$R_{m_0} = R^*\left(1 + \sqrt{\frac{\alpha_m}{\alpha_t}}\right) - \alpha_m T^*. \tag{8}$$

This allows us to obtain for $R_t(T)$

$$R_t(T) = R^*\left(1 + \sqrt{\frac{\alpha_t}{\alpha_m}}\right) - \alpha_t(T - T^*), \tag{9}$$

and for $R_m(T)$

$$R_m(T) = R^*\left(1 + \sqrt{\frac{\alpha_m}{\alpha_t}}\right) + \alpha_m(T - T^*), \tag{10}$$

allowing us to arrive at an expression for the equivalent resistance $R(T)$:

$$R(T) = R^* - \frac{\sqrt{(\alpha_m\alpha_t)^3}(T - T^*)^2}{R^*(\sqrt{\alpha_m} + \sqrt{\alpha_t})^2 + (\alpha_m - \alpha_t)\sqrt{\alpha_m\alpha_t}(T - T^*)}. \tag{11}$$

It is clear from Eq. (11) that, as expected, at $T=T^*$ one has $R=R^*$ and that this point is a maximum of the expression. We further notice that, given the data point (T^*,R^*), the above expression depends on only two parameters (α_m and α_t). If $\alpha_t=\alpha_m=\alpha$, one finds $R(T)=R^*-\frac{\alpha^2(T-T^*)^2}{4R^*}$; i.e., we have a parabola centered at T^*. Thus, for similar α_t and α_m coefficients, we expect a closely symmetric curve. The larger the differences between the $\alpha_{m,t}$ values, the more asymmetric shall this curve be.

Before proceeding, note that the four model parameters (R_{t_0}, R_{m_0}, α_t, and α_m) also depend on the MTJ magnetic state ($\sigma \equiv$ P, AP), as experimentally observed. In fact, measurements on tunnel junctions with thick MgO barriers always show a $R(T)$ behavior that is quite insensitive to temperature when the MTJ is in the parallel state ($dR^{\mathrm{P}}/dT \sim 0$), but large resistance variations for the antiparallel state ($dR^{\mathrm{AP}}/dT < 0$), so that $\alpha^{\mathrm{AP}} \gg \alpha^{\mathrm{P}}$ (e.g., we have measured $\alpha^{\mathrm{P}} \approx 0.5\ \Omega/\mathrm{K}$ and $\alpha^{\mathrm{AP}} \approx 5.2\ \Omega/\mathrm{K}$ in MgO tunnel junctions with $t=13$ Å for which a low-temperature TMR of $\sim$240% was obtained and estimated, $\alpha^{\mathrm{P}} \approx 0.13$ kΩ/K and $\alpha^{\mathrm{AP}} \approx 1$ kΩ/K from Ref. 37, for $t=15$ Å). On the other hand, for current perpendicular to the plane spin valves, we have estimated a much smaller dependence of the α parameters on the spin valve state ($\alpha^{\mathrm{P}} \approx 1.222$ mΩ/K and $\alpha^{\mathrm{AP}} \approx 1.216$ mΩ/K).[30] We will show below that when one considers such behaviors, a wealth of different $R(T)$ variations can be observed depending also on the MTJ magnetic state.

V. DISCUSSION

We can now fit our experimental $R(T)$ data using the developed model. Figure 5(a) shows the fit to Eq. (11) of the

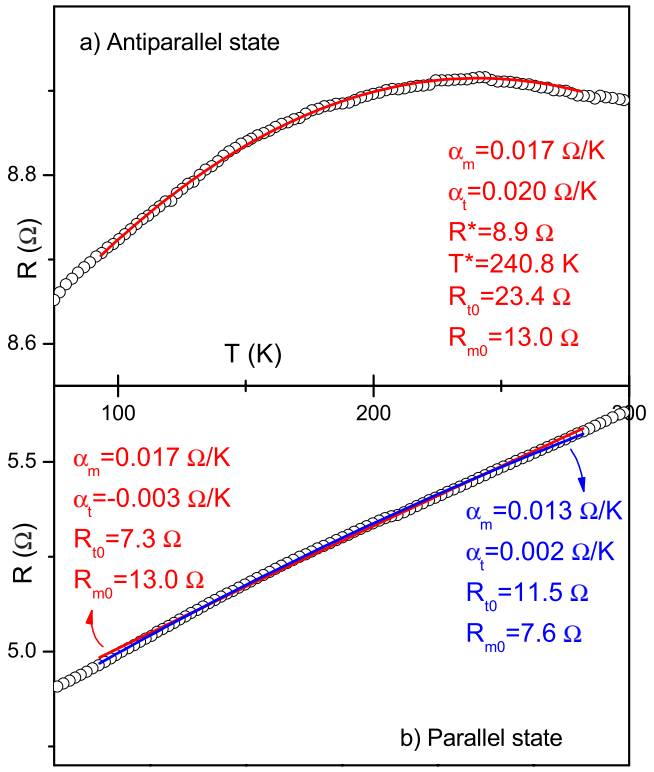

FIG. 5. (Color online) (a) Fits of the $R^{AP}(T)$ curve of sample 2 using the developed model [Eq. (11)]. (b) Fits to the $R^{P}(T)$ curve of sample 2 using the two procedures described in the text.

R^{AP} curve of sample 2. We observe that the fit reproduces the experimental data quite well, particularly if we take into account the simplicity of the model. We obtained the following parameters for the antiparallel state (see also Table I): $R_{t_0}^{AP}=23.4\ \Omega$, $R_{m_0}^{AP}=13.0\ \Omega$, $\alpha_t^{AP}=20.0\ \mathrm{m\Omega/K}$, and $\alpha_m^{AP}=17.0\ \mathrm{m\Omega/K}$.

One can now fit the curve of the parallel state using one of two procedures. First, we can consider that the metallic paths have no MR and then the obtained metallic parameters do not depend on the MTJ magnetic state (so that $R_{m_0}^{AP}=R_{m_0}^{P}=13.0\ \Omega$ and $\alpha_m^{AP}=\alpha_m^{P}=17.0\ \mathrm{m\Omega/K}$). This two-parameter fitting procedure leads to good agreement between fit and experimental curve [Fig. 5(b)]. From the obtained fitting parameters one notices that: (i) the calculated value of the tunnel magnetoresistance (MR_{t_0} in Table I) is very large (220%) and (ii) the value of α_t^{P} is negative, indicating that the tunneling resistance in the parallel state increases with temperature, contrary to what has always been observed in magnetic tunnel junctions without pinholes. The same overall behavior is also observed for sample 1 (Table I), for which a TMR $\sim 195\%$ is calculated.

Such negative sign in α_t^{P} obliged us to consider an alternative fit where all four parameters ($R_{t_0}^{P}$, $R_{m_0}^{P}$, α_t^{P}, and α_m^{P}) are used, leading also to a good correlation with experiment [Fig. 5(b)]. In this case we find $\alpha_t^{P}>0$, which corresponds to the usual decrease in the tunneling resistance with increasing temperature and we find that the tunnel magnetoresistance is substantially smaller than that obtained using the alternative fitting procedure. Furthermore, the obtained metallic parameters are different from those of the antiparallel state, strikingly indicating that a magnetoresistive mechanism (MR_{m_0} in Table I) occurs through the metallic pinholes across the barrier.

The obtained metallic magnetoresistance may arise from several mechanisms. Spin-dependent transport across pinholes was recently claimed in $La_{0.67}Sr_{0.33}MnO_3/Ba_2LaNbO_6/La_{0.67}Sr_{0.33}MnO_3$ tunnel junctions.[8] In fact, electron transport through thin domain walls at a nanocontact can be analogous to tunneling in MTJs, since both depend equally on the FM electrode spin polarization.[31,39] Thus, one cannot distinguish between (spin-dependent) currents arising from tunneling or from pinholes based on MR measurements alone. Furthermore, a very large MR enhancement was also recently observed in current confined path spin valves,[40,41] with an AlCu oxidized spacer. A thin AlO_x layer is then formed with embedded narrow conductive Cu channels. It was shown that transport through these Cu nanoconstrictions displays enhanced spin-dependent interface scattering.[40]

Notice that a crossover from positive to negative dR/dT of the *parallel* state should also be visible at a sufficiently high temperature when one considers the second fitting procedure. In fact, using Eqs. (5) and (6), one calculates a T^* crossover temperature above 1000 K for both samples (values in parentheses in Table I). Although this would allow a definitive confirmation of the correct fitting procedure, the calculated crossover temperature is high enough to induce structural damage in the studied system.

Finally, we note that a total of five different samples of this series ($t=7.5$ Å) were measured as a function of tem-

TABLE I. Obtained fitting parameters for the antiparallel state (first and fourth rows), parallel state using only two fitting parameters (second and fifth rows), and parallel state using four fitting parameters (third and sixth) for samples 1 and 2. Values of T^* and R^* in parentheses were calculated using Eqs. (5) and (6).

Sample	State	T^* (K)	R^* (Ω)	α_m (Ω/K)	α_t (Ω/K)	R_{m_0} (Ω)	R_{t_0} (Ω)	MR_{t_0} (%)	MR_{m_0} (%)
	AP	89.8	8.56	0.0185	0.0153	16.3	17.7		
1	P			0.0185	−0.001	16.3	6.00	195	0
	P	(1042)	(5.13)	0.013	0.001	10.1	7.6	132	61
	AP	240.8	8.9	0.017	0.020	13.0	23.4		
2	P			0.017	−0.003	13.0	7.3	220	0
	P	(1200)	(6.54)	0.013	0.002	7.6	11.5	103	71

perature (with RA values ranging from ~ 10 to 50 $\Omega\mu m^2$ and $R \sim 1.2-7.5$ Ω). Positive dR^P/dT and a crossover from positive to negative dR^{AP}/dT with increasing temperature were observed for all these samples. Samples 1 and 2 presented here have the highest and lowest T^* values of the measured samples. All $R(T)$ curves could be fitted by the developed model, revealing MR_{m_0} values between 60% and 80%.

VI. CONCLUSIONS

We have studied the temperature dependence (300–20 K) of the transport properties of low resistance MTJs ($RA \sim 40$ $\Omega\mu m^2$) with a thin MgO barrier (7.5 Å) and TMR of $\sim 60-75$ % at room temperature. Our $R(T)$ measurements showed different behaviors depending on the MTJ magnetic state. We have observed positive dR/dT (metalliclike behavior) for the P state in the studied temperature range and samples, which means that pinholes are already present in the barrier. On the other hand, a transition from negative to positive dR/dT was observed in the AP state as temperature decreases. This transport behavior was well described by the proposed simple model. We found that T^* depends strongly on the linear temperature coefficients for the metallic (α_m) and tunnel (α_t) channels. Simulated results show that increasing α_m leads to the increase in T^*, while for increasing α_t, T^* decreases. These results were obtained for a metallic conductance much higher than the tunnel conductance. This indicates that the sign of dR/dT does not give an indication of the dominant conductance mechanism. The validity of the model was confirmed by fitting our experimental $R(T)$ data with the model equations, allowing us to observe that the fits reproduce the experimental data quite well. Our analysis shows that a metallic spin-dependent transport channel can occur through pinhole nanoconstrictions.

ACKNOWLEDGMENTS

This work was supported in part by Grant Nos. FEDER-POCTI/0155, PTDC/CTM/73263/2006, and POCTI/CTM/59318/2004 from FCT and Project No. IST-2001-37334 NEXT MRAM. The authors acknowledge funding from FCT through the Associated Laboratory–IN. J.M.T. is thankful for a FCT grant (No. SFRH/BD/24012/2005). P.W. acknowledges the financial support provided through the European Community's Marie Curie actions (Research Training Networks) under Contract No. MRTN-CT-2003-504462 (ULTRASMOOTH).

*joventur@fc.up.pt

[1] J. S. Moodera, L. R. Kinder, T. M. Wong, and R. Meservey, Phys. Rev. Lett. **74**, 3273 (1995).
[2] E. Y. Tsymbal, O. N. Mryasov, and P. R. LeClair, J. Phys.: Condens. Matter **15**, R109 (2003).
[3] S. Mao, J. Nanosci. Nanotechnol. **7**, 1 (2007).
[4] S. Mao *et al.*, IEEE Trans. Magn. **42**, 97 (2006).
[5] J. G. Zhu, J. Appl. Phys. **97**, 10N703 (2005).
[6] J. Ventura, R. Ferreira, J. B. Sousa, and P. P. Freitas, IEEE Trans. Magn. **42**, 2658 (2006).
[7] G. Finocchio, G. Consolo, M. Carpentieri, A. Romeo, B. Azzerboni, L. Torres, and L. Lopez-Diaz, Appl. Phys. Lett. **89**, 262509 (2006).
[8] S. Mukhopadhyay and I. Das, Phys. Rev. Lett. **96**, 026601 (2006).
[9] S. Yuasa and D. D. Djayaprawira, J. Phys. D **40**, R337 (2007).
[10] C. Tiusan, F. Greullet, M. Hehn, F. Montaigne, S. Andrieu, and A. Schuhl, J. Phys.: Condens. Matter **19**, 165201 (2007).
[11] S. S. P. Parkin, C. Kaiser, A. Panchula, P. M. Rice, B. Hughes, M. Samant, and S. H. Yang, Nat. Mater. **3**, 862 (2004).
[12] S. Yuasa, T. Nagahama, A. Fukushima, Y. Suzuki, and K. Ando, Nat. Mater. **3**, 868 (2004).
[13] S. Yuasa, A. Fukushima, H. Kubota, Y. Suzuki, and K. Ando, Appl. Phys. Lett. **89**, 042505 (2006).
[14] Y. M. Lee, J. Hayakawa, S. Ikeda, F. Matsukura, and H. Ohno, Appl. Phys. Lett. **90**, 212507 (2007).
[15] W. H. Butler, X.-G. Zhang, T. C. Schulthess, and J. M. MacLaren, Phys. Rev. B **63**, 054416 (2001).
[16] J. Mathon and A. Umerski, Phys. Rev. B **63**, 220403(R) (2001).
[17] Y. Nagamine, H. Maehara, K. Tsunekawa, D. D. Djayaprawira, N. Watanabe, S. Yuasa, and K. Ando, Appl. Phys. Lett. **89**, 162507 (2006).
[18] K. Tsunekawa, D. D. Djayaprawira, M. Nagai, H. Maehara, S. Yamagata, N. Watanabe, S. Yuasa, Y. Suzuki, and K. Ando, Appl. Phys. Lett. **87**, 072503 (2005).
[19] E. Burstein and S. Lundqvist, *Tunneling Phenomena in Solids* (Plenum, New York, 1969).
[20] B. J. Jönsson-Åkerman, R. Escudero, C. Leighton, S. Kim, I. K. Schuller, and D. A. Rabson, Appl. Phys. Lett. **77**, 1870 (2000).
[21] J. J. Akerman, R. Escudero, C. Leighton, S. Kim, D. A. Rabson, R. W. Dave, J. M. Slaughter, and I. K. Schuller, J. Magn. Magn. Mater. **240**, 86 (2002).
[22] B. Oliver, Q. He, X. Tang, and J. Nowak, J. Appl. Phys. **94**, 1783 (2003).
[23] J. Ventura, Z. Zhang, Y. Liu, J. B. Sousa, and P. P. Freitas, J. Phys.: Condens. Matter **19**, 176207 (2007).
[24] J. Ventura, J. P. Araujo, J. B. Sousa, R. Ferreira, and P. P. Freitas, Appl. Phys. Lett. **90**, 032501 (2007).
[25] R. J. Pedersen and F. L. Vernon, Appl. Phys. Lett. **10**, 29 (1967).
[26] J. Ventura, J. P. Araujo, J. B. Sousa, A. Veloso, and P. P. Freitas, J. Appl. Phys. **101**, 113901 (2007).
[27] J. Ventura, J. P. Araujo, J. B. Sousa, A. Veloso, and P. P. Freitas, Phys. Rev. B **77**, 184404 (2008).
[28] X. Kou, J. Schmalhorst, A. Thomas, and G. Reiss, Appl. Phys. Lett. **88**, 212115 (2006).
[29] S. Kim, H. Suhl, and I. K. Schuller, Phys. Rev. Lett. **78**, 322 (1997).
[30] F. Delille, A. Manchon, N. Strelkov, B. Dieny, M. Li, Y. Liu, P. Wang, and E. Favre-Nicolin, J. Appl. Phys. **100**, 013912 (2006).
[31] M. Julliere, Phys. Lett. **54A**, 225 (1975).
[32] C. H. Shang, J. Nowak, R. Jansen, and J. S. Moodera, Phys. Rev. B **58**, R2917 (1998).

[33] A. H. MacDonald, T. Jungwirth, and M. Kasner, Phys. Rev. Lett. **81**, 705 (1998).
[34] L. Yuan, S. H. Liou, and D. Wang, Phys. Rev. B **73**, 134403 (2006).
[35] S. Zhang, P. M. Levy, A. C. Marley, and S. S. P. Parkin, Phys. Rev. Lett. **79**, 3744 (1997).
[36] X. F. Han, A. C. C. Yu, M. Oogane, J. Murai, T. Daibou, and T. Miyazaki, Phys. Rev. B **63**, 224404 (2001).
[37] V. Drewello, J. Schmalhorst, A. Thomas, and G. Reiss, Phys. Rev. B **77**, 014440 (2008).
[38] J. O. Ventura, J. B. Sousa, M. A. Salgueiro da Silva, P. P. Freitas, and A. Veloso, J. Appl. Phys. **93**, 7690 (2003).
[39] N. Garcia, Appl. Phys. Lett. **77**, 1351 (2000).
[40] H. Fukuzawa, H. Yuasa, S. Hashimoto, H. Iwasaki, and Y. Tanaka, Appl. Phys. Lett. **87**, 082507 (2005).
[41] H. Fuke, S. Hashimoto, M. Takagishi, H. Iwasaki, S. Kawasaki, K. Miyake, and M. Sahashi, IEEE Trans. Magn. **43**, 2848 (2007).